Experience with the EM-60 electromagnetic system for geothermal exploration in Nevada

M. Wilt*, N. E. Goldstein*, M. Stark‡, J. R. Haught§, and H. F. Morrison§

ABSTRACT

Lawrence Berkeley Laboratory (LBL) conducted controlled-source electromagnetic (EM) surveys at three geothermal prospects in northern Nevada to test and demonstrate the applicability of LBL's EM-60 system to geothermal exploration. During the late summer and early fall of 1979, over 40 soundings were made in Panther Canyon (Grass Valley), near Winnemucca; Soda Lakes, near Fallon; and McCoy, west of Austin.

The EM-60 is a frequency-domain system using three-component magnetic detection. For the surveys reported here, we applied ±65 A to a 100-m diameter four-turn horizontal loop, generating a dipole moment $>10^6$ mks over the frequency range 10^{-3} to 10^3 Hz. With such a source loop and a remote magnetic reference for noise cancellation, we made soundings at transmitter-receiver separations of up to 4 km over the frequency range of 0.05 to 500 Hz. This has yielded a maximum depth of exploration to 2 km or more, adequate for the purposes of the geothermal investigations. Recorded spectra are interpreted by means of simple apparent-resistivity calculations made in the field and by layered-model inversions computed in the laboratory. The EM interpretations are then compared with other available geologic/geophysical data sets for the purpose of combined interpretation and method evaluation. Experience with the EM-60 system in Nevada has shown it to be an efficient and possibly more cost-effective alternative to dc resistivity and magnetotellurics for geothermal exploration. An average of two soundings per field day for depths of exploration up to 2 km was obtained routinely.

Results from EM-60 work at Panther Canyon compare very favorably with earlier dipole-dipole resistivity surveys. Both methods outlined an irregularly shaped, buried conductive body associated with a region of high heat flow, but the feature was delineated by means of the EM-60 in just over half the field time required for the dipole-dipole resistivity survey. At Soda Lakes, 13 high-quality EM soundings were obtained from two transmitters in six field days under ideal field conditions. With the EM-60 data, we were able to map the depth to and inclination of a buried conductive body associated with an area of high subsurface temperatures. In this case, the EM results confirmed an earlier MT survey interpretation and gave additional detailed near-surface information. At the remote and mountainous McCoy site, data interpretation was complicated because of the rugged terrain. By modifying existing interpretive software, we were able to calculate the effects of tilted-source dipoles and elevation differences on soundings and thus interpret data. The EM soundings detected a conductive zone at a depth of 200 m at the south end of the prospect, where a nearby drillhole had encountered water at 100°C at the same depth. In addition, EM soundings at McCoy provided information on a deep conductor below 2 km which has yet to be drilled.

INTRODUCTION

In 1976, Lawrence Berkeley Laboratory, in conjunction with the University of California at Berkeley, made preliminary measurements with a prototype horizontal-loop electromagnetic (EM) prospecting system near Leach Hot Springs in Grass Valley, Nevada (Jain, 1978). Encouraging results from this work led to the development of the frequency-domain EM-60 horizontal-loop system, which has now been operated for over 500 hours at several geothermal sites in Nevada and Oregon (Morrison et al, 1978). The objectives of LBL's controlled-source EM program are to develop new hardware and software tools for geothermal exploration and to demonstrate the technical feasibility and cost-effectiveness of the technique.

The EM method offers two significant advantages in geothermal exploration: (1) the maximum depth of exploration with EM is approximately equal to the distance between the transmitter and

receiver (for dc resistivity, almost five times the source-receiver separation is required for the same depth of exploration); and (2) distant lateral inhomogeneities, which often affect MT data, have relatively minor effects on EM data because the strength of the fields decreases sharply with increasing distance from the transmitter.

As part of the DOE-Industry Coupled Case Studies Program for the northern Basin and Range Province, LBL conducted EM-60 surveys at three geothermal target areas in northern Nevada: Panther Canyon in Grass Valley; Soda Lakes, near Fallon; and McCoy, west of Austin (Figure 1). These areas were chosen on the basis of industry interest, access to land, and, to some extent, availability of other geologic and geophysical data. This paper summarizes the significant findings in each area; more complete descriptions, including field data and layered-model inversions, are given in Stark et al (1980) and Wilt et al (1980a, b).

EM-60 SYSTEM DESCRIPTION

With the EM-60 system, the earth is energized by means of an alternating magnetic field created by a square-wave current applied to a horizontal loop (Figure 2). Power is provided by a Hercules gasoline engine linked to a 60 kW, 400 Hz aircraft alternator; the two components are mounted on the bed of a 1-ton four-wheel-drive truck (Figure 3). The alternator output is full-wave rectified
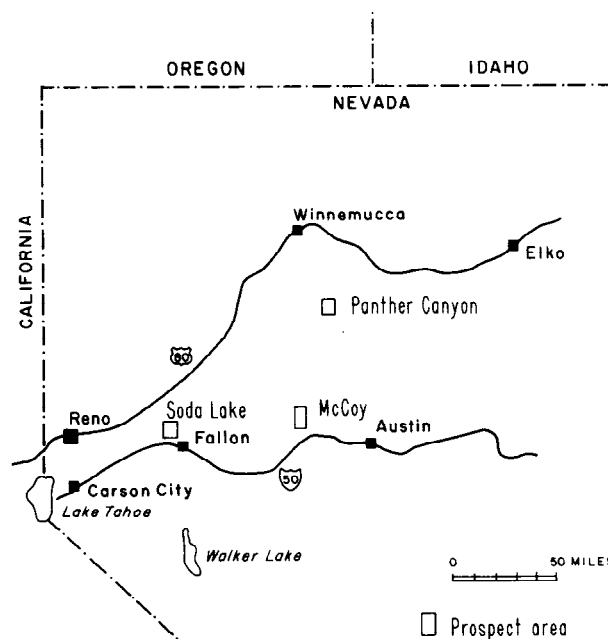

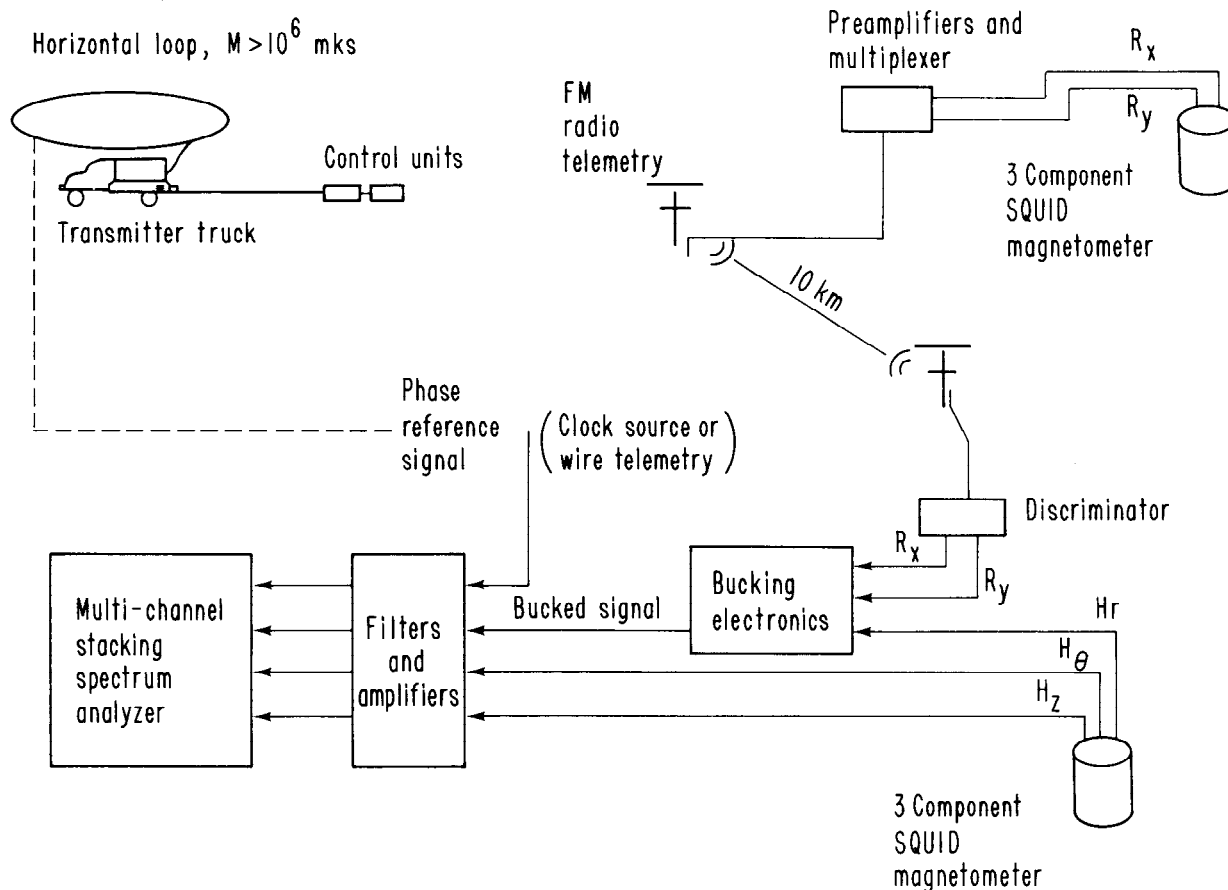FIG. 1. Location map for the three EM-60 surveys conducted in 1979 by LBL.

FIG. 2. Schematic diagram of the EM-60 horizontal-loop prospecting system as used in Nevada in 1979.

FIG. 3. The EM-60 transmitter.

and capable of providing ±150 V at up to 400 A to the loop[1], although in practice we have never approached this current. The current waveform is created with a transistorized switch, which consists of two parallel arrays of 6 to 60 transistors mounted in sets of three in interchangeable modules (Morrison et al, 1978). The operator remotely sets the fundamental frequency of the current waveform; four frequencies per decade are switch selectable. The fundamental frequencies are generated by means of a crystal-controlled oscillator over the range of 10^{-3} to 10^3 Hz.

The dipole moment, which is a measure of the primary field strength, is a function of the resistance and inductance of the loop. At frequencies below about 50 Hz, a four-turn, 50-m radius loop of 6-gauge wire will yield a dipole moment of 3×10^6 mks. Except in very conductive terrain this provides adequate signal for transmitter-receiver separations less than about 4 km. Above 50 Hz the loop inductance reduces the moment and causes the current waveform to become quasi-sinusoidal. Because of the reduced moment, high-frequency information becomes more difficult to obtain at larger transmitter-receiver separations. The 50-m loop has proven satisfactory for most geothermal operations: it can be laid out from a truck in about 30 minutes, and it provides sufficient power for exploration depths of up to 4 km. If greater depth of penetration is required, larger loops and/or heavier gauge wire can be used. However, to achieve a two-fold increase of exploration depth, an approximate four-fold increase in source strength is required and logistical problems associated with the greater weight and length of wire must be considered.

[1] The system has since been modified to operate at a voltage of +250 V, providing a 60 percent larger current for the same loop parameters.

Magnetic fields were detected at receiver sites with a three-component SQUID magnetometer oriented to measure the vertical, radial, and tangential components with respect to the loop. Electric dipoles may also be used in combination with or instead of magnetic sensors. Signals are amplified and antialias filtered before input to a six-channel, programmable, phase-sensitive receiver. Through the receiver key pad, the operator sets the parameters that control signal processing: (a) fundamental period of the waveform to be processed; (b) maximum number of harmonics to be analyzed, up to 15; (c) number of cycles to be stacked prior to Fourier decomposition; and (d) number of input channels of data to be processed. Processing results in a raw amplitude estimate for each component and a phase estimate relative to the phase of the current in the source loop. Raw amplitude estimates must later be corrected for dipole moment and distance and elevation difference between loop and magnetometer. In the original system, phase referencing was done by carrying a reference voltage via a hard-wire link between a shunt resistor on the loop and channel 1 on the receiver. In practice, the hard-wire link was found to be a source of noise, particularly above 50 Hz. We consequently eliminated the absolute phase reference at high frequencies in favor of relative phase measurements between vertical and radial components. With relative phase measurements, interpretation is based on the ellipticity and tilt angle of the combined magnetic fields rather than amplitude-phase spectra of the vertical and radial fields. Recently, high-precision, synchronous quartz clocks have been added for phase reference permitting us to obtain absolute phase information up to 1 kHz.

At low frequencies (<1.0 Hz), natural geomagnetic signal

amplitude increases roughly as $1/f$, and the secondary (induced) magnetic field decreases as $1/f$. The net result is an effective signal-to-noise (S/N) ratio that decreases as $1/f^2$. High levels of geomagnetic noise can therefore be a formidable barrier to obtaining low-frequency information, particularly on the horizontal component channels. To reduce the effect of geomagnetic noise, a second (reference) magnetometer is placed at a convenient location far enough from the transmitter loop (usually about 10 km) that the observed remote fields consist only of the geomagnetic fluctuations (Figure 2). Placed at a properly chosen site, the reference magnetometer need not be relocated during the course of a survey. The horizontal magnetic fields R_x and R_y at the remote site are transmitted to the mobile receiver station from the reference station via FM radio telemetry. Before the loop is energized, the remote signals are inverted, adjusted in amplitude, and then added by scalar addition to the receiver station geomagnetic signal to produce essentially a null signal. Once the loop is energized, the resulting magnetic signals processed are virtually free of geomagnetic noise. A graphic illustration of the results of this simple noise cancellation scheme is shown in Figure 4. The resulting S/N improvement of roughly 20 dB has allowed us to obtain reliable data to 0.05 Hz, an addition of three or four important data points on the sounding curve. These points are of great value for resolving deeper horizons. This noise cancellation scheme has reduced low-frequency averaging times by a factor of 4 and has allowed us to obtain low-frequency information even at high geomagnetic noise levels.

DATA INTERPRETATION

Apparent resistivity function

Apparent resistivity versus frequency curves can be calculated from EM spectra by matching observed field data to generalized, homogeneous half-space curves (Wilt and Stark, 1982). The generalized curves are a plot of spectral field value versus induction number B, which is a function of the frequency, transmitter-receiver separation, and resistivity of the half-space. A resistivity spectrum can therefore be obtained by matching observed data to the generalized curve and calculating the conductivity from the induction number. For a multilayered section, an apparent resistivity curve is obtained from this calculation.

An example of such a curve calculated from a three-layer model is given in Figure 5; calculations for each type of measured data reflect the layered-model section shown at the bottom, although there is scatter between the curves. The curves are generally used for qualitative interpretation. They give asymptotic values for earth resistivities and indicate the resistivity type section, thus allowing more accurate "first guesses" for the layered-model inversion algorithm. The curves are also useful for evaluating data quality in the field and for isolating noisy data for deletion prior to inversion.

Layered-model inversion

Quantitative interpretation is accomplished by least-squares inversion of observed data to fit one-dimensional (1-D) models. Layered-model forward solutions may be calculated for a finite-loop source or for a point dipole source (Ryu et al, 1970; Anderson, 1979). The loop-source solution is perfectly general and is more accurate when soundings are made close to the source. The point-dipole solution is calculated using digital filters and is identical to the loop solution for transmitter-receiver separations greater than ten loop radii. Since the digital filter calculation is much less expensive, the point-dipole source is normally used in the layered-

A. NATURAL MAGNETIC
FIELD CANCELLATION
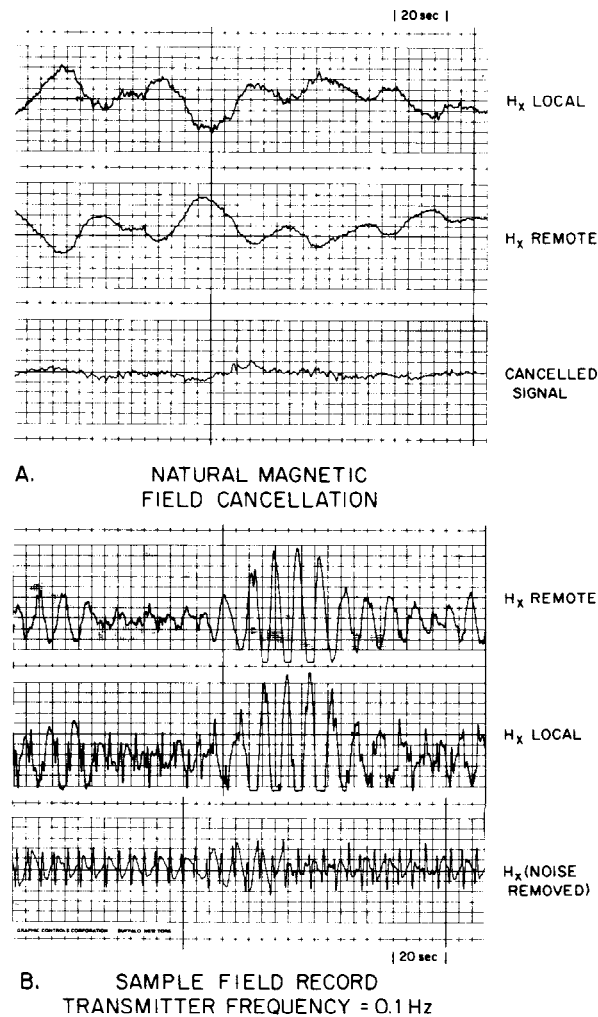
B. SAMPLE FIELD RECORD
TRANSMITTER FREQUENCY = 0.1 Hz

FIG. 4. Example of data improvement using the telluric noise cancellation scheme. (a) Natural geomagnetic signal and initial cancelling at the receiver site with transmitter off. (b) Same system with transmitter on.
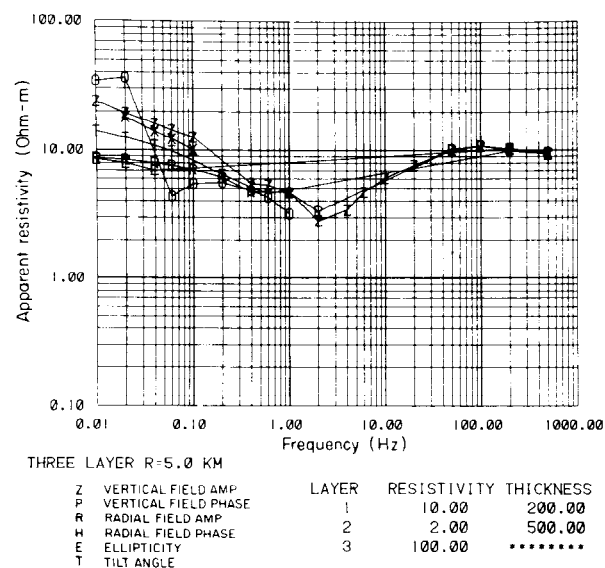

THREE LAYER R = 5.0 KM

		LAYER	RESISTIVITY	THICKNESS
Z	VERTICAL FIELD AMP	1	10.00	200.00
P	VERTICAL FIELD PHASE			
R	RADIAL FIELD AMP	2	2.00	500.00
H	RADIAL FIELD PHASE			
E	ELLIPTICITY	3	100.00	••••••
T	TILT ANGLE			

FIG. 5. EM apparent resistivity spectra calculated from layered-model theoretical data.

COMPARISON OF CALCULATED AND MEASURED DATA

COMPARISON OF CALCULATED AND MEASURED DATA

SODA LAKE .72 KM NW T1

CALCULATED DATA	MEASURED DATA		LAYER	RESISTIVITY(OHM-M)		THICKNESS(M)	
HR ———————	HR	X	1	12.11*	.00	305.4	* 2.
HZ — — — —	HZ	*	2	1.77*	.02	.1000E-11*	0.

DATA VARIANCE ESTIMATE 15.23
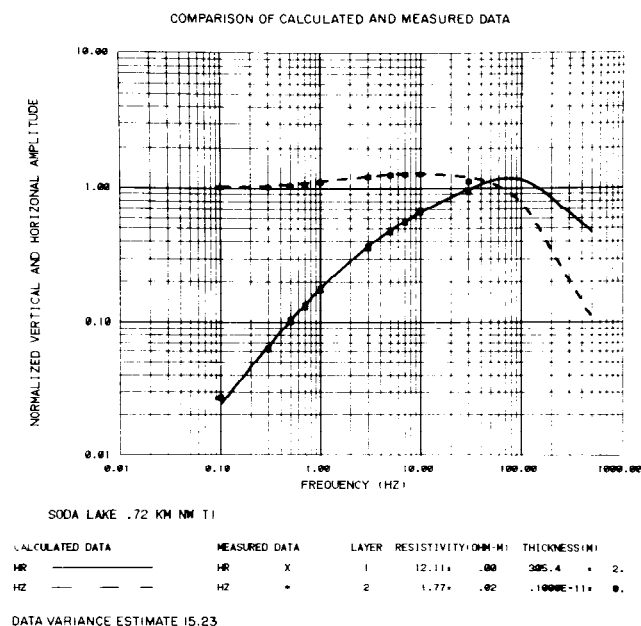
FIG. 6. Examples of the EM-60 vertical and horizontal amplitude spectra and their fit to a two-layer model.

SODA LAKE .72 KM NW T1

CALCULATED DATA	MEASURED DATA		LAYER	RESISTIVITY(OHM-M)		THICKNESS(M)	
ELLIPTICITY ———————	ELLIPTICITY	X	1	12.11*	.00	305.4	* 2.
			2	1.77*	.02	.1000E-11*	0.

DATA VARIANCE ESTIMATE 15.23

FIG. 7. Example of an EM-60 ellipticity spectrum and its fit to a two-layer model.

model inversion program. The inversion program uses the Marquardt least-squares algorithm to fit amplitude-phase and/or ellipse polarization parameters jointly or separately to layered models (Inman, 1975). This program allows the use of polarization parameters to fit the high-frequency points where absolute phase data are noisier and simultaneously use absolute phase data to fit the lower frequencies where the phase reference allows for better parameter resolution. Observed data are weighted by the standard deviation of field measurements. These are accurate representations of true error if noise sources are random. When sources are nonrandom (which is the usual case) the error estimates are probably somewhat low, thus leading to low estimates of parameter errors.

Our experience indicates that 1-D interpretation seems to give adequate results. Because of the rapid fall-off in field strength with distance, dipole fields seem to be much less affected by nearby lateral discontinuities and current channeling which, for example, impair 1-D MT interpretations. Although we rely mainly on 1-D interpretations, 2-D forward modeling of dipole EM data may be done for special cases (Lee, 1978). The finite-element program used for 2-D calculations is very expensive and cumbersome, however, and the model considered must be fairly simple to yield an accurate solution. The program is used chiefly for theoretical studies, although it has been used occasionally to help interpret field data affected by severe two- or three-dimensional geology.

An example of a layered-model inversion for an EM-60 sounding is given in Figures 6 and 7. The vertical and radial amplitude and ellipticity spectra shown are three of the six spectra normally calculated for a field sounding, the others being vertical and radial phase and tilt angle. The data were fitted jointly to the two-layer model shown at the bottom of each figure. Note that because of noise associated with the hardwire link, good amplitude data were obtained only up to 30 Hz, but good ellipticity data were obtained to 500 Hz.

In areas of rugged terrain it may be necessary to lay out the transmitter loop on a inclined surface. For this condition, the source
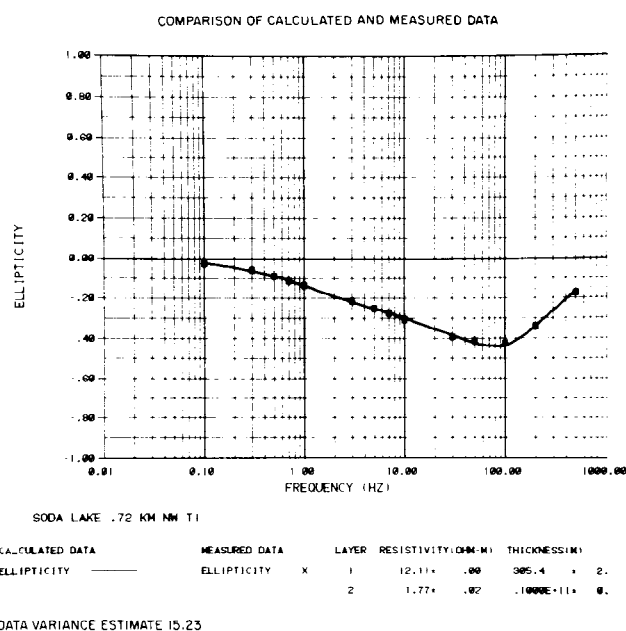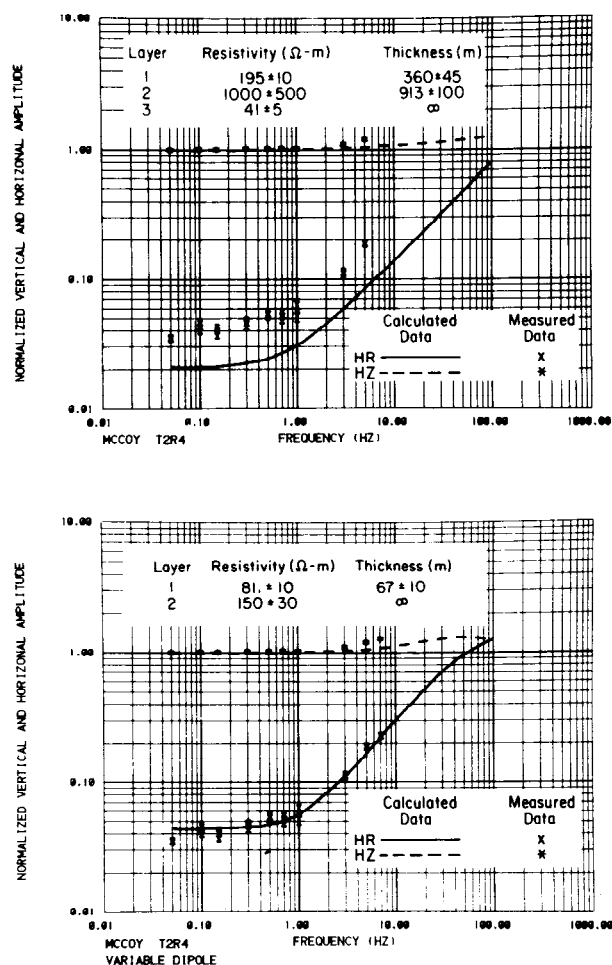

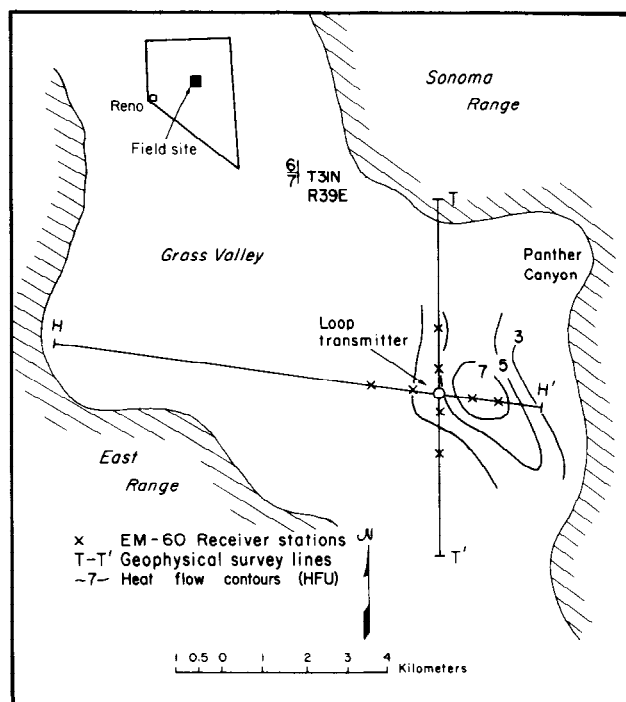FIG. 8. Comparison of inversions from a vertical dipole source (top) and a tilted dipole source (bottom).

FIG. 9. Location of the EM stations in the Panther Canyon area, Grass Valley, Nevada with respect to the heat flow anomaly.

Panther Canyon

Panther Canyon is located in the southeastern corner of Grass Valley, a northerly trending Basin and Range valley in north-central Nevada (Figure 9). The region is characterized by high heat flow (Sass et al, 1977), active hot springs (Olmsted et al, 1975), and recent faulting (Noble, 1975; Majer, 1978).

As part of a detailed investigation of the geothermal potential of Grass Valley, LBL performed reconnaissance and detailed geophysical surveys throughout the region. Work has included dipole-dipole resistivity and telluric profiling (Beyer, 1977), magneto-telluric sounding (Morrison et al, 1979), passive seismics (Majer, 1978), gravity (Goldstein and Paulsson, 1978), and heat flow (Sass et al, 1977). Composite profiles and a preliminary synthesis of some of these data are given in Beyer et al (1976).

Geothermal interest in Panther Canyon was heightened after several shallow boreholes indicated anomalously high heat flow values (7 HFU, or about three times the regional average). Subsequent telluric profile and dipole-dipole resistivity studies revealed a low-resistivity zone at depth beneath the heat flow high, thus suggesting the presence of geothermal waters at depth. The region

dipole must be treated as the sum of a vertical and a horizontal dipole, rather than the purely vertical dipole that is considered in the idealized, flat-earth case. To interpret field data properly for an inclined dipole, Haught et al (1981) developed a computer program to calculate EM fields over a layered earth from an arbitrarily oriented dipole. The program combines layered-model solutions for vertical and horizontal dipoles at the appropriate strength and orientation to calculate the correct magnetic fields at the receiver sites. The solution was used in a least-squares inversion routine, and trials of the program provided good results at a reasonable cost.

An example of the effect of the tilted dipole is given in Figure 8, which shows two interpretations for a set of EM sounding data obtained at the McCoy field area from a tilted dipole. The upper graph shows our attempt to interpret the data, assuming a vertical dipole. Of the various two- or three-layer models that we considered, the one that gives the best fit is a three-layer section that indicates the presence of a conductor at about 1.3 km in depth. The bottom of Figure 8 shows a layered model fit for a two-layer section with a tilted dipole source. Here the fit is superior, and with no indication of a deeply buried conductor. This example illustrates how ignoring even small inclinations at the source dipole (1 degree in this case) can give misleading results. This is particularly true in regions of high resistivity, such as McCoy, where the secondary magnetic fields are sensitive to small tilts of the source dipole.

FIELD SURVEYS WITH THE EM-60 SYSTEM

In the sections below, we give a summary of significant findings of field surveys taken in central Nevada during the summer and fall of 1979. For each project we summarize the known geology, geophysics, and drilling history, and we interpret EM sounding data in light of this information.
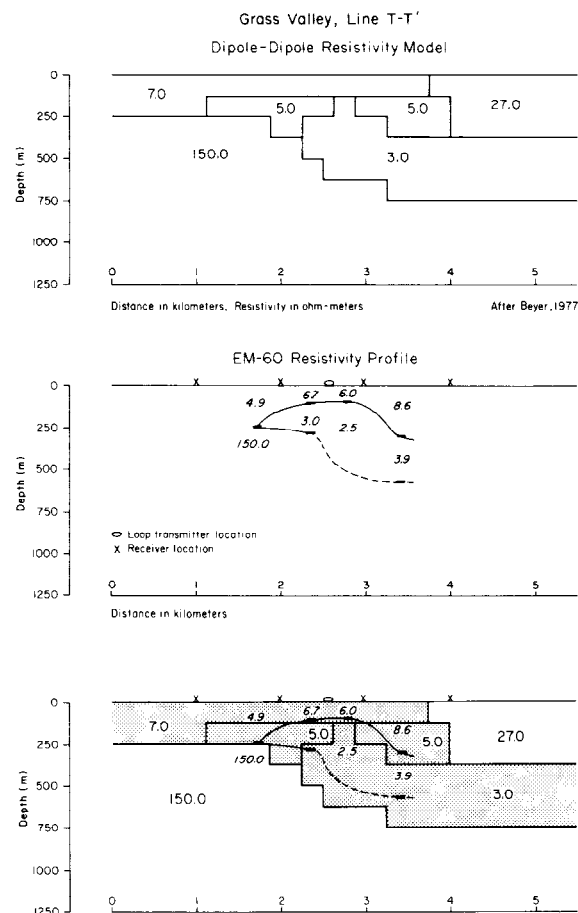

FIG. 10. Resistivity cross-section over line in Panther Canyon: (a) two-dimensional dipole-dipole resistivity model; (b) profile of one-dimensional EM-60 electromagnetic soundings; and (c) comparison of (a) and (b).

was also found to be seismically active (Majer, 1978), with swarm-type activity along a northeast-southwest fault aligned with Panther Canyon. Electromagnetic soundings were made over the heat flow anomaly near the Panther Canyon area for the purpose of comparison to existing dipole-dipole and telluric data. The EM-60 field survey consisted of eight soundings arranged along two orthogonal lines crossing at the transmitter loop; transmitter-receiver separations ranged from 400 to 1600 m. The EM stations are located along survey lines used previously for the dipole-dipole survey (Figure 9).

Electromagnetic sounding data from Panther Canyon were interpreted by individual layered-model inversions of spectra; best-fit

models were then pieced together along the profile, and sections were plotted at a distance halfway from the source to the receiver. Good data were collected at all sites, and reasonable models were obtained from inversions.

Figure 10 is a north-south resistivity cross-section over the Panther Canyon thermal anomaly. The figure gives a comparison of a 2-D model made from dipole-dipole resistivity data and the composite resistivity section made from EM sounding results. At first glance, the interpretations are remarkably similar. Both cross-sections indicate resistive surface material overlying an irregular southward-dipping conductive body. Depth to resistive basement is shown to vary between 250 and 800 m below the surface. The
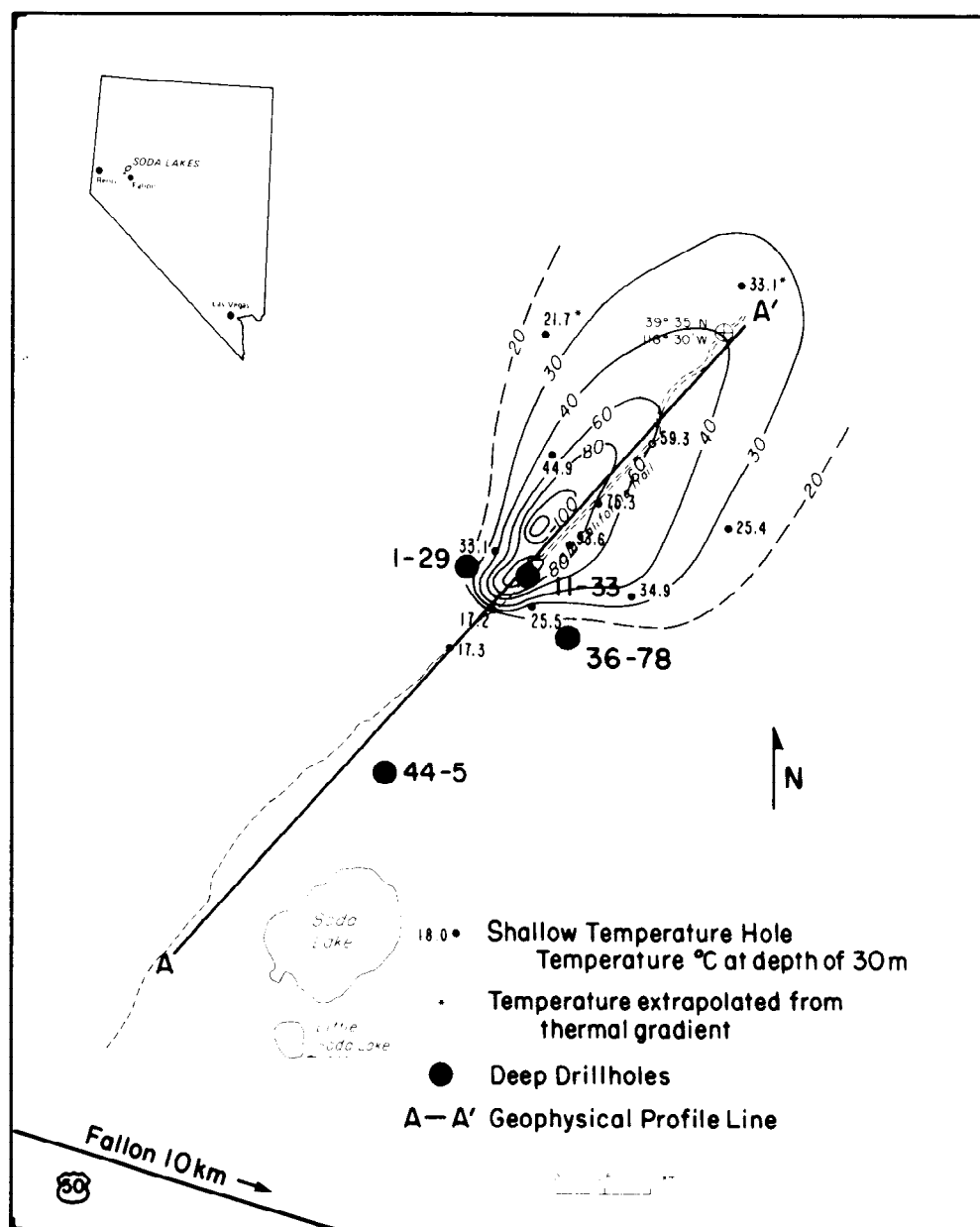

FIG. 11. Location map and shallow temperature survey results, Soda Lakes geothermal anomaly.

depth to the conductive body associated with the thermal anomaly is well resolved by both methods. The two profiles disagree somewhat on the depth to resistive basement beneath the conductor. Because the EM method is less sensitive to resistive formations, and because the transmitter-receiver separations were more than five times greater with the dipole-dipole data, the conventional resistivity section is probably more accurate in determining this parameter. The crossing east-west profile indicates that the conductive body is narrow and dips steeply westward. The outline of the conductor is therefore roughly similar to the heat flow contours, forming an ellipse with the major axis parallel to the adjacent north-south-trending range front. These results indicate that the observed conductor could be a warm-water aquifer with fault-controlled recharge to the east along the border of the range front. To date, however, no deep drilling in this area has been done.

Soda Lakes

Soda Lakes geothermal anomaly is located about 8 miles northwest of Fallon within the Carson Sink of west-central Nevada (Figure 11). The Carson Sink is a large depression filled with unconsolidated sediments to a depth of at least 6000 ft (Garside and Schilling, 1979). The Soda Lakes area is characterized by flat to hummocky topography, numerous small lake beds, and several small basaltic volcanic manifestations of Quaternary age. Soda Lake and Little Soda Lake fill explosion craters, probably formed within the past 10,000 years (Garside and Schilling, 1979). The geothermal anomaly, located 5 km north of Soda Lake, was discovered accidentally in 1903 when drillers found boiling water at a depth of 60 ft in a water well. A recent shallow temperature survey of the region by the U.S. Geological Survey has revealed
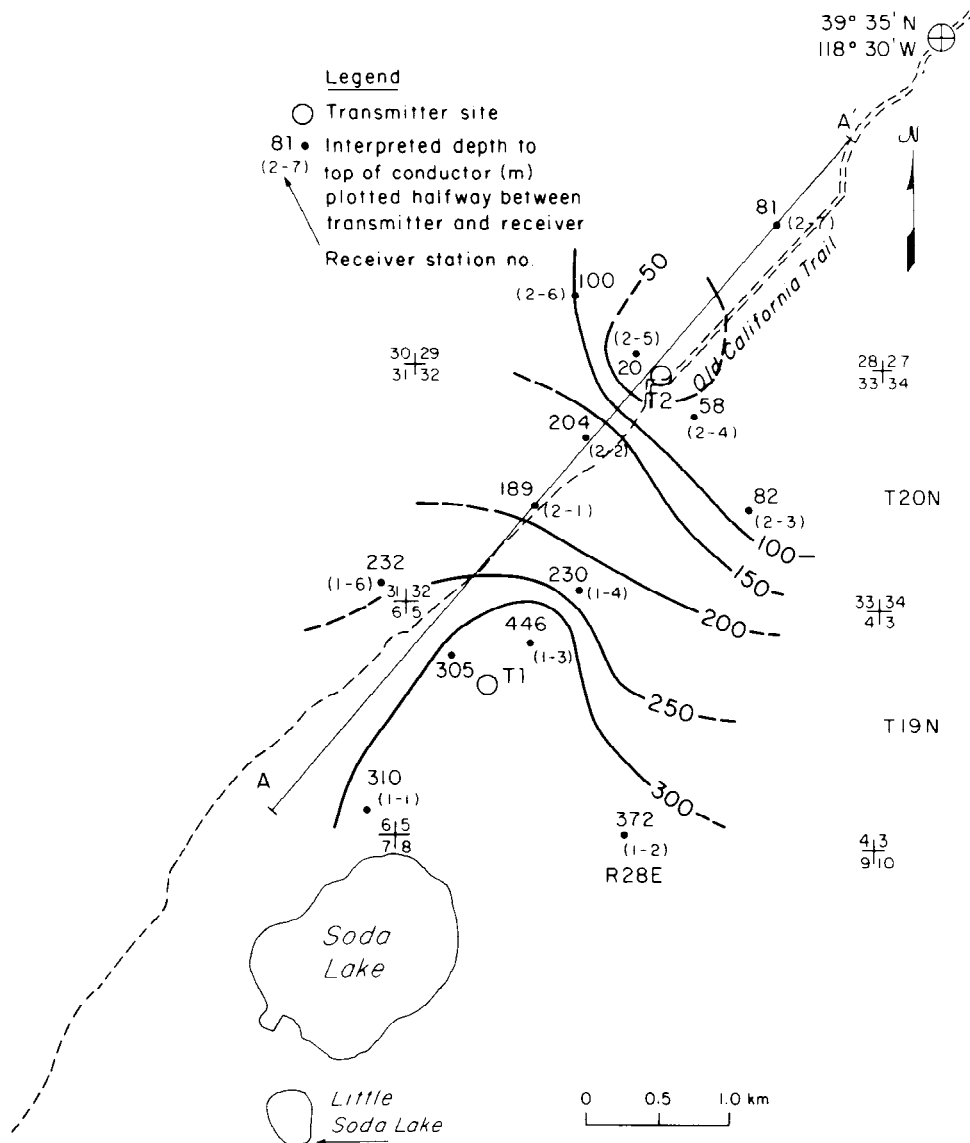

Fig. 12. Contours on interpreted depth to the top of conductive second layer, Soda Lakes geothermal anomaly.

high temperatures over a 5 km² area (Figure 11). Temperature contours are elongated to the northeast, which is the direction of regional groundwater flow (Olmsted et al, 1975).

Magnetotelluric soundings, dipole-dipole resistivity surveys, and reflection seismic surveys have all been conducted in the Soda Lakes region; in addition, three deep exploratory wells have been drilled. Data obtained during these surveys were made available to LBL by Chevron Resources, Inc., as part of the DOE-Industry Coupled Program.

Dipole-dipole resistivity data and MT soundings indicate that the subsurface may be approximated by a three- or four-layer section. The top layer is approximately 10 Ω-m in resistivity and varies from 100 to 400 m in thickness. The second layer is 2 Ω-m or less in resistivity and 400 to 1000 m in thickness. Well logs show that the top layer consists predominantly of sand and the second predominantly of shale. Higher temperatures and some evidence of hydrothermal alteration are observed locally in the second layer, and in some areas the geothermal activity may be partly responsible for the low resistivity. For most of the region the predominant cause for the low resistivity is probably the brine saturated shaly sequence. MT soundings show a high-resistivity basement at a depth of 1 to 2 km. Well logs indicate that the

upper part of this layer consists mostly of sandstone and volcaniclastic and volcanic rocks. MT data also show a regional conductor at a depth of nearly 10 km but coming to within only 3 km of the surface beneath Soda Lake. This decrease in depth of the deep conductor is as yet unexplained. A seismic reflection survey indicates the predominance of northeast-trending normal faulting in the area and suggests that the thermal anomaly lies within a deep northeast-trending graben. The seismic data also show numerous shallow northwest-trending faults with displacements of a few meters. At the time of the EM-60 survey, three deep geothermal wells had been drilled (Figure 9). None of these was a good producer, but temperatures in excess of 170°C at 700 m depth were reported in well 11-33 in the vicinity of the shallow temperature maximum (Hill et al, 1979) (Figure 11).

The EM survey at Soda Lakes was made to obtain EM sounding data for comparison with other data. The survey consisted of 13 soundings from 2 transmitter loops with transmitter-receiver separations ranging from 500 m to about 3 km (Figure 12). Good quality data were collected at all sites within a one-week period by a crew of four. The survey was designed to map the configuration of the conductive layer associated with high temperatures. The interpreted depth to the top of this conductive layer is shown in Figure 12. EM station coverage included areas near existing boreholes so that interpretations could be compared with well data. A series of soundings was made along a northeast-trending profile (A-A') connecting deep test wells so that subsurface structure could be mapped between the wells.

Figure 13 is a resistivity cross-section comparing 1-D EM interpretations, 1-D MT interpretations, and lithologic logs from wells along the profile A-A'. The EM and MT resistivity cross-sections are remarkably similar, both indicating a three-layer section with similar layer parameters. The sections differ most near the southwestern end where the MT data indicate a shallow basement layer and the EM data show no basal resistive layer. Since there are no drill holes in this region and no other geophysical data, the discrepancy remains unresolved. Both methods indicate a shallowing and thinning of the conductive second layer near wells 1–29 and 11–33. The EM data show a significant resistivity decrease in the second layer near these wells that may be due to an increase in temperature or the presence of hot fluid. EM soundings also suggest that a northwest-trending fault in this region is controlling the shallow thermal system. The offset on this fault is not clear, however, since the resistivity boundaries do not match well with the lithologic units.

McCoy

The remote and mountainous McCoy region is located about 40 miles west of Austin, within the Augusta and Clan Alpine mountain ranges. Geologically, the area is characterized by Tertiary volcanics overlying Mesozoic and Paleozoic sedimentary and metamorphic rocks. Several mercury deposits within the volcanics have been mined. There are no surface thermal discharges, but a 2 km² fossilized travertine mound near the McCoy mercury mine indicates former geothermal activity (Figure 14). When the EM survey was conducted, Amax, Inc., the principal leaseholder, was at an early stage of prospect evaluation. Some temperature gradient surveying, self-potential measurements, and water sampling had been done, but few other data were available to supplement the EM results. Temperature gradient measurements indicated a 100 km² region of anomalously high thermal gradients within which three maxima were located (Figure 14). Self-potential (SP) measurements show elongation of contours in a northwesterly direction, although there are indications of dipolar-type anomalies near a thermal gradient maximum at the
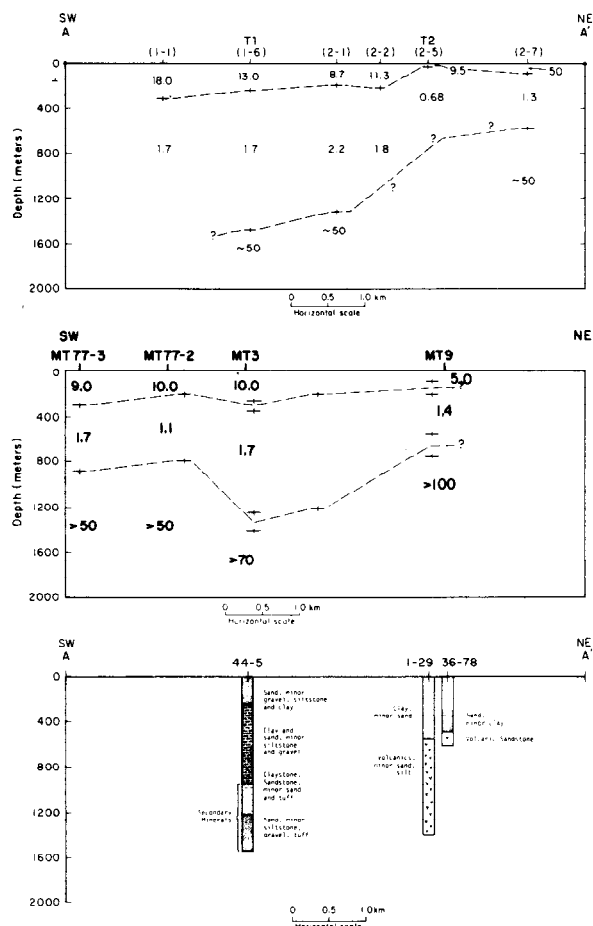

FIG. 13. (a) Interpreted EM resistivity cross-section; (b) interpreted MT resistivity cross-section; and (c) generalized lithologic logs for three wells (bottom) along profile A-A'.
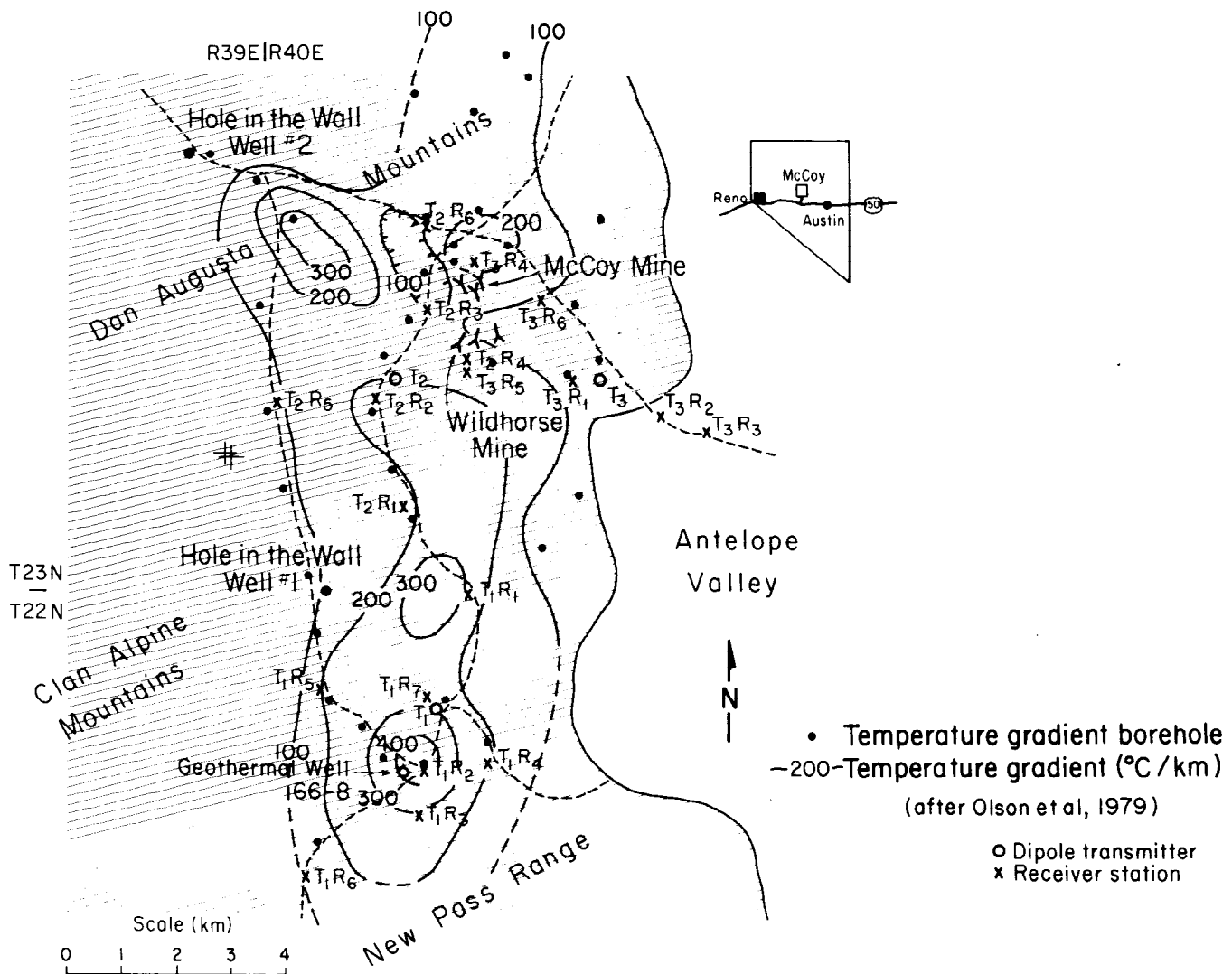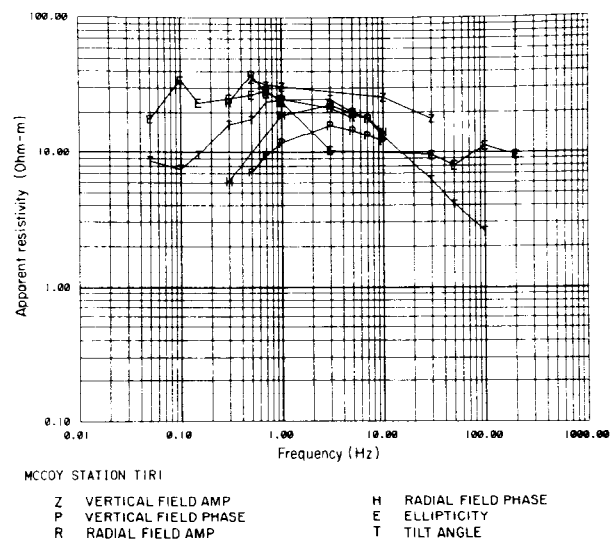
FIG. 14. Temperature gradient map of the McCoy region.

McCoy mine and near geothermal well 66–8. Dipolar SP anomalies have been linked to active geothermal systems in several cases (Corwin and Hoover, 1979).

Nineteen EM soundings were made at McCoy from three loop transmitters; transmitter-receiver separations ranged from 400 m to more than 4050 m. The survey was designed such that north-south and east-west trending sections could be made from interpreted soundings. The McCoy area provided significant challenges for crew and equipment. Because the area is mountainous and access is difficult, soundings could only be made in selected areas. Moreover, there were few flat places on which to lay out the transmitter loops, and therefore most soundings were made from inclined loops, making data interpretation much more difficult. For most stations there was a significant difference between transmitter and receiver elevations. This made it imperative to determine correct elevations for proper interpretation; the effect of the intervening topography could not, however, be determined.

We constructed apparent resistivity spectral plots to obtain an initial model for use in the inversion program and for qualitative interpretation of well-behaved sounding data. The apparent re-

MCCOY STATION T1R1

Z	VERTICAL FIELD AMP	H	RADIAL FIELD PHASE
P	VERTICAL FIELD PHASE	E	ELLIPTICITY
R	RADIAL FIELD AMP	T	TILT ANGLE

FIG. 15. Apparent resistivity spectral plot for EM station T_1R_1.

sistivity curves can be used effectively only if there is no elevation difference between source and receiver and no tilting of the transmitter dipole. Only 4 of the 19 soundings at McCoy, all from transmitter 1, satisfy these criteria.

Figure 15 is an apparent resistivity spectral plot for station $T_1 R_1$. The figure shows apparent resistivity values plotted for all six types of data. There is considerable agreement in the shape of the curves, but substantial scatter among values calculated for each parameter. The curves suggest a three-layer section consisting of a conductive surface layer, a resistive intermediate layer, and a conductive deeper layer. Apparent resistivity plots for stations located closer to the transmitter indicate a resistive surface layer. Combining the apparent resistivity plots, we find evidence for a four-layer section for the region near transmitter 1. This basic section was successfully tried on layered-model inversions for this area.

Figure 16 is a north-south resistivity cross-section made from interpreted EM soundings located near the southern thermal gradient maximum and geothermal test well 66–8. The section gives resistivities and depths of the various layers as well as an elevation profile. The soundings generally indicate a three- or four-layer section which includes a shallow conductive layer and a resistive deeper layer. The layered interpretation for sounding $T_1 R_2$ appears somewhat different from interpretations for adjacent soundings; the surface layer is more resistive and the deeper (third) layer is more conductive. A likely explanation is that this station is located on a bluff overlooking the transmitter and topographic effects may be causing some distortion. We cannot, however,

account for topographic graphic effects in calculations.

The section indicates that the surface layer is generally resistive and probably represents undersaturated Tertiary flows and tuffs. Shallow wells in this area indicate that the water table depth exceeds 100 m (Olson et al, 1979). The depth of the shallow conductive layer corresponds well to that of a zone of warm-water inflow marked in geothermal test well 66–8 and is probably indicative of a shallow, warm-water aquifer. Within the high-resistivity Mesozoic section beneath this shallow conductor, sounding $T_1 R_6$ indicated a deep conductor. This deeper layer is as yet unexplored by drill holes, but recent MT results show a conductor at a similar depth in the same area, confirming the EM results (Lange, 1980). Additional exploration and some deep geothermal reservoir is a possibility, however.

CONCLUSIONS

The EM-60 electromagnetic system was used at three different geothermal prospects in northern Nevada. For the most part the system performed very well; two soundings per day were easily possible, and interpretable data were obtained at all sites. The field work demonstrated fundamental strengths and weaknesses of EM induction techniques. The system achieved good depth of penetration and was operable in rough terrain. The tests also demonstrated the ability of the EM-60 to locate buried conductive bodies accurately. The limitations lie in the present difficulty of interpretation using 2-D and 3-D computer modeling and in the insensitivity of the technique to resistive bodies. Until improved computer algorithms are developed, 2-D and 3-D interpretations
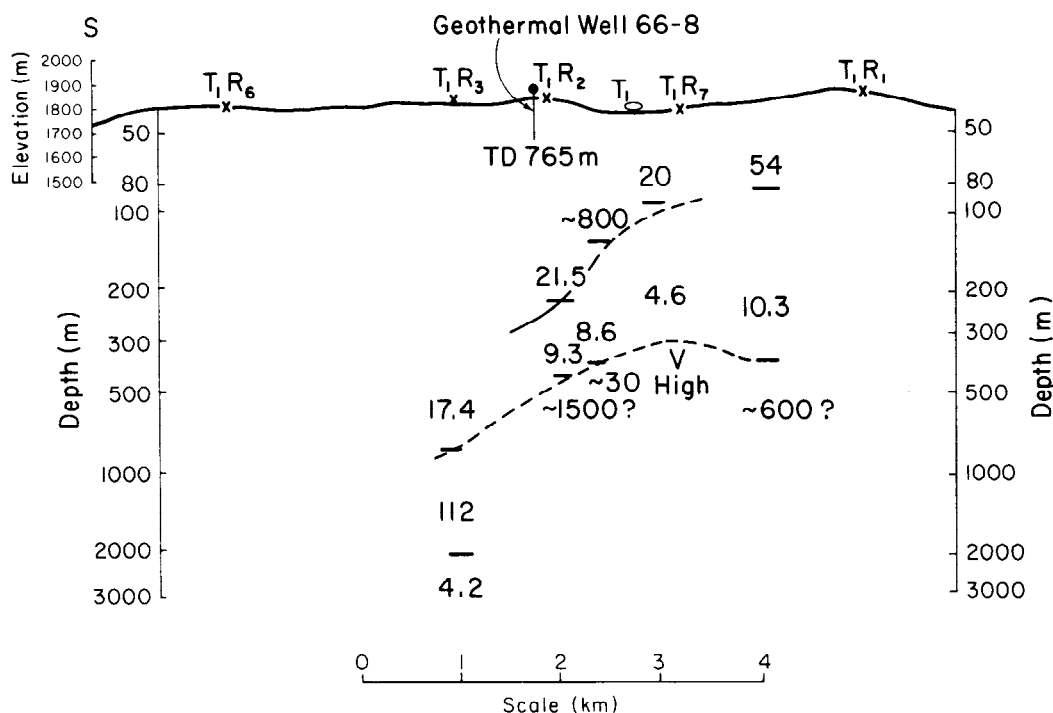

FIG. 16. North-south profile of interpreted EM soundings over the McCoy prospect. Layered-model parameters, resistivity (Ω-m) and depth (m) are plotted at points midway between source and receiver positions.

will be impractical. However, because of the spatial decaying of the source field, 1-D interpretations seem to be providing useful results.

Although the method is in an early stage of development, our experience has indicated that it has the potential to become a powerful exploration tool. Future applications may include basin studies, petroleum exploration, and large-scale geothermal prospecting.

ACKNOWLEDGMENTS

REFERENCES

Anderson, W. L., 1979, Numerical investigation of related Hankel transforms of orders 0 and 1 by adaptive digital filtering: Geophysics, v. 44, p. 1287–1305.

Beyer, J. H., 1977, Telluric and dc resistivity techniques applied to the geophysical investigation of Basin and Range geothermal systems, part III: The analysis of data from Grass Valley, Nevada: Lawrence Berkeley Laboratory, LBL-6325.

Beyer, J. H., Dey, A., Liaw, A., Majer, E., McEvilly, T. V., Morrison, H. F., and Wollenberg, H. A., 1976, Preliminary open file report—Geological and geophysical studies in Grass Valley, Nevada: Lawrence Berkeley Laboratory, LBL-5262.

Corwin, R. F., and Hoover, D. B., 1979, The self-potential method in geothermal exploration: Geophysics, v. 44, p. 226–245.

Garside, L. J., and Schilling, J. H., 1979, Thermal waters of Nevada: Nevada Bur. Mines and Geol., Bull. 91.

Goldstein, N. E., and Paulsson, B., 1978, Interpretation of gravity surveys in Grass and Buena Vista Valleys, Nevada: Geothermics, v. 7, p. 29–50:

Haught, J. R., Wilt, M. J., and Goldstein, N. E., 1981, Deep induction sounding for geothermal exploration from an arbitrarily oriented magnetic dipole (abstr.); Geophysics, v. 46, p. 458.

Hill, D. G., Layman, E. B., Swift, C. M., and Yungul, S. H., 1979, Soda Lake, Nevada, thermal anomaly, *in* Expanding the geothermal frontier: Trans., Geothermal Resources Council Annual Meeting, v. 3, p. 305–308.

Inman, J. R., 1975, Resistivity inversion with ridge regression: Geophysics, v. 40, p. 798–817.

Jain, B., 1978, A low-frequency eleectromagnetic prospecting system: Ph.D. dissertation, Univ. of California, Berkeley and Lawrence Berkeley Laboratory, LBL-7042.

Lange, A. L., 1980, The McCoy, Nevada geothermal prospect: An interim case history. Presented at the 50th Annual International SEG Meeting, in Houston.

Lee, K. H., 1978, Electromagnetic scattering by a two-dimensional inhomogeneity due to an oscillating magnetic dipole: Ph.D. dissertation, Univ. of California, Berkeley and Lawrence Berkeley Laboratory, LBL-8275.

Majer, E., 1978, Seismological investigations in geothermal areas: Ph.D. dissertation, Univ. of California, Berkeley and Lawrence Berkeley Laboratory, LBL-7054.

Morrison, H. F., Goldstein, N. E., Hoversten, N., Oppliger, G., and Riveros, C., 1978, Description, field test and data analysis of controlled source EM system (EM-60): Lawrence Berkeley Laboratory, LBL-7088.

Morrison, H. F., Lee, K. H., Oppliger, G., and Dey, A., 1979, Magnetotelluric studies in Grass Valley, Nevada: Lawrence Berkeley Laboratory, LBL-8646.

Noble, D. C., 1975, Geologic history and geothermal potential of the Leach Hot Springs area, Pershing County, Nevada: Preliminary report to Lawrence Berkeley Laboratory.

Olmsted, F. H., Glancy, P. A., Harrill, J. R., Rush, F. E., and Van Denburgh, A. S., 1975, Preliminary hydrologic appraisal of selected hydrothermal systems in northern and central Nevada: U.S.G.S. open-file rep. 75–56.

Olson, H. J., Dellechaie, F., Pilkington, H. D., and Lange A., 1979, The McCoy geothermal prospect status report of a possible new discovery in Churchill and Lander Counties, Nevada, *in* Expanding the geothermal frontier: Trans., Geothermal Resources Council Annual Meeting, v. 3, p. 515–519.

Ryu, J., Morrison, H. F., and Ward, S. H., 1970, Electromagnetic fields about a loop source of current: Geophysics, v. 35, p. 862–896.

Sass, J. H., Siagos, J. P., Wollenberg, H. A., Munroe, R. J., DiSomma, D., and Lachenbruch, A. H., 1977, Application of heat flow techniques to geothermal energy exploration, Leach Hot Springs, Grass Valley, Nevada: Lawrence Berkeley Laboratory, LBL-6809.

Stark, M., Wilt, M., Haught, J. R., and Goldstein, N. E., 1980, Controlled source electromagnetic survey at Soda Lakes geothermal area, Nevada: Lawrence Berkeley Laboratory, LBL-11221.

Wilt, M., Haught, R., and Goldstein, N. E., 1980a, An electromagnetic (EM-60) survey of the McCoy geothermal prospect, Nevada: Lawrence Berkeley Laboratory, LBL-12012.

Wilt, M., Goldstein, N., Stark, M., and Haught, R., 1980b, An electromagnetic EM-60 survey in Panther Canyon area, Grass Valley, Nevada: Lawrence Berkeley Laboratory, LBL-10993.

Wilt, M., and Stark, M., 1982, A simple method for calculating apparent resistivity from electromagnetic sounding data: Geophysics, v. 47, p. 1100.